CHEMISTRY
A European Journal

Accepted Article

Authors: Lianke Wang, Matija Zlatar, Filip Vlahovic, Serhiy Demeshko, Christian Philouze, Florian Molton, Franc Meyer, Carole Duboc, Maja Gruden, and Marcello Gennari

WILEY-VCH

COMMUNICATION

Experimental and Theoretical Identification of the Origin of Magnetic Anisotropy in Intermediate Spin Iron(III) Complexes.

Lianke Wang,[a] Matija Zlatar,[b] Filip Vlahović,[c] Serhiy Demeshko,[d] Christian Philouze,[a] Florian Molton,[a] Marcello Gennari,[a] Franc Meyer,[d] Carole Duboc*[a] and Maja Gruden*[c]

Abstract: The complexes [FeL^{N2S2}X] (where L^{N2S2} = 2,2'-bipryridine-6,6'-diyl)bis(1,1'-diphenylethanethiolate) and X = Cl, Br and I), characterized crystallographically earlier and here (**Fe(L)Br**), reveal a square pyramidal coordinated Fe^{III} ion. Unusually, all three complexes have intermediate spin ground states. Susceptibility measurements, powder *cw* X- and Q-band EPR spectra, and zero-field powder Mössbauer spectra show that all complexes display distinct magnetic anisotropy, which has been rationalized by DFT calculations.

Predicting and rationalizing the electronic and magnetic properties of transition metal ions is a core challenge in coordination chemistry. This is particularly important for complexes that exhibit non-standard ground states, such as intermediate spin systems. The latter are relatively uncommon but critically important in, for example, the study of spin-cross-over processes, single ion single-molecule magnets, and in (enzymatic) catalysis.[1] In the case of Fe^{III} (d^5), intermediate spin ground states are observed mainly for complexes of square pyramidal coordination geometry with few exceptions found in octahedral or square planar complexes in case of suitable ligand environments.[2] Although the electronic and magnetic properties of a number of mononuclear S = 3/2 Fe^{III} complexes have been the subject of detailed experimental studies, the corresponding computational studies are limited to the determination of the spin of their ground states, and, to the best of our knowledge, the present report is the first theoretical consideration of the origin of their magnetic anisotropy.[1a, 1d, 3]

Here we report a series of closely related mononuclear square pyramidal Fe^{III} complexes that display an intermediate spin ground state, and we take advantage of this unique opportunity to carry out combined experimental and theoretical studies that are essential to develop a rational correlation between their structural and magnetic properties.

The [FeL^{N2S2}X] complexes (with L^{N2S2} = 2,2'-(2,2'-bipyridine-6,6'-diyl)bis(1,1'-diphenylethanethiolate) and X = Cl, Br and I), **Fe(L)Cl**, **Fe(L)Br** and **Fe(L)I**, were isolated following the reaction of L^{N2S2} with FeX$_3$ (X = Cl[4] and Br) in tetrahydrofuran (THF) or between the dinuclear Fe^{II} disulfide complex **Fe^{II}$_2$SS**[5] and an excess of tetra-n-butylammonium iodide in acetonitrile (MeCN) for **Fe(L)I** (Scheme 1). The structures of **Fe(L)Br** and **Fe(L)I** is reported in Figure S1.1, while the structure of **Fe(L)Cl**[4] was reported earlier. All three complexes are obtained with a penta-coordinated iron center in a distorted square pyramidal geometry (τ_5 value of 0.328 in **Fe(L)Cl**, 0.317 in **Fe(L)Br** and 0.291

in **Fe(L)I**) with the halide occupying the apical position and the N2S2 donor atoms of L^{N2S2} constituting the equatorial plane. All Fe-N/S distances and valence angles are similar, however an expected difference arises from the Fe-X distances (2.313 Å in **Fe(L)Cl**, 2.473 Å in **Fe(L)Br** and 2.673 Å in **Fe(L)I**) in agreement with the different ionic radii of the halides (see S1). This is compensated by a variation of the position of the iron ion with respect to the mean equatorial plane formed by the N2S2 atoms. The iron ion resides 0.537, 0.512 and 0.476 Å out of this plane towards the axial chlorido, bromide and iodido ligands, respectively. The long Fe…Fe distances observed in each crystal demonstrate that the three mononuclear Fe^{III} complexes are magnetically isolated species (the shortest Fe…Fe distance: 8.965, 8.868 and 8.958 Å, in **Fe(L)X**, X = Cl, Br, I, respectively).
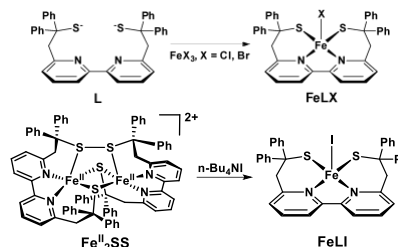
Scheme 1. Synthesis of **Fe(L)X** (X=Cl, Br, I)

The temperature dependence of the χT product for **Fe(L)Br** and **Fe(L)I** is shown in Figure 1 together with that of **Fe(L)Cl** for comparison. The room temperature χT values for all complexes are consistent with the expected values for S = 3/2 species. This is also confirmed by Density Functional Theory (DFT) calculations performed at OPBE[6] and S12g[7]/TZ2P level of theory, which was shown to be accurate for spin state energetics.[8] Separate optimizations for the three possible spin states (low, intermediate, high) reported in Table 1 show clearly that the intermediate-spin state, S=3/2, is in all cases the spin ground state, whereas the order of excited states depends on the level of theory (Table S3.1). The geometries of optimized S=3/2 complexes are in excellent agreement with X-ray structures, with an r.m.s. error of less than 1.3 pm (Table S3.2, Figure S3.1).

Table 1. Spin state energetics (kcal/mol^{-1}) of **Fe(L)X** (X=Cl, Br, I) relative to intermediate spin ground state calculated using two different levels of theory

	S	Fe(L)Cl	Fe(L)Br	Fe(L)I
	LS[*] [(**)] 1/2	7.7	7.4	6.4
OPBE/TZ2P	IS[*] 3/2	0.0	0.0	0.0
	HS[*] 5/2	5.5	6.3	7.5
	LS[*] [(**)] 1/2	7.8	7.7	6.2
S12g/TZ2P	IS[*] 3/2	0.0	0.0	0.0
	HS[*] 5/2	5.3	6.1	7.0

[*] LS- low spin, IS- intermediate spin, HS- high spin
[**] Spin projection technique (both for the energy and the gradients) to correct the spin contamination has been used.

[a] Lianke Wang, Dr. Christian Philouze, Florian Molton and Dr. Carole Duboc*
University of Grenoble Alpes, DCM,
CNRS UMR 5250,
Grenoble, France
E-mail: carole.duboc@univ-grenoble-alpes.fr
[b] Dr. Matija Zlatar
Institute of Chemistry, Technology and Metallurgy
University of Belgrade
[c] Filip Vlahović and Prof. Maja Gruden*
Faculty of Chemistry
University of Belgrade
Studentski trg 12–16, 11000 Belgrade, Serbia
E-mail: gmaja@chem.bg.ac.rs
[d] Dr. Serhiy Demeshko and Prof. Franc Meyer
Universität Göttingen
Institut für Anorganische Chemie
Tammannstr. 4, D-37077 Göttingen, Germany

Supporting information for this article is given via a link at the end of the document

COMMUNICATION

The intermediate spin ground state is a consequence of strong and covalent bonding in the xy plane, and weak bonding between the metal ion and the axial ligand. Hence, the $d_{x^2-y^2}$ orbital is the highest in energy and well separated from the other four metal-based orbitals, including the d_{z^2} orbital. At the same time, nephelauxetic reduction due to the covalency decreases pairing energy, leading to the double occupation of the mainly non-bonding d_{xy} orbital, and thus to an S=3/2 ground state (Figures S3.2 and S3.3).

The magnetic properties of an S=3/2 system, such as the present **Fe(L)X** complexes, can be described by a Spin Hamiltonian that includes the zero field splitting (ZFS) terms and the electronic Zeeman interaction (Equation (1)).

$$\hat{H} = D\left[\hat{S}_z^2 - \frac{1}{3}S(S+1) + \frac{E}{D}(\hat{S}_x^2 - \hat{S}_y^2)\right] + g\mu_B\vec{B}\cdot\vec{S} \qquad \text{Equation (1)}$$

with S being the spin, D and E the axial and rhombic ZFS parameters and g the isotropic electronic Zeeman interaction.

The magnetic susceptibilities of the complexes remain constant down to ca. 30 K. At lower temperatures, the χT values decrease, as expected for moderate ZFS. Powder cw X- and Q-band EPR spectra recorded at low temperatures (5-30 K) display features at low field corresponding to transitions between the Kramers doublet $M_S = \pm 3/2$ (Figures S2.1-2). E/D values of 0.18, 0.13 and 0.12 (Table 2) were estimated for **Fe(L)Cl**, **Fe(L)Br** and **Fe(L)I**, respectively, from the detailed analysis of the spectra (S2 and Figures S2. 3-5). The E/D decrease from **Fe(L)Cl** to **Fe(L)I** is consistent with the distortion around the Fe center that increases concomitant with the τ_5 values. The temperature dependence of $\chi_M T$ and variable temperature-variable field (VTVH) magnetization data were simultaneously fitted using these E/D values to estimate the D values, 3.7, 5.2 and 11.5 cm^{-1} for **Fe(L)Cl**, **Fe(L)Br** and **Fe(L)I**, respectively (Table 2). The trend, i.e. an increase of D with the increase of the halide SOC, is generally observed[9] in mononuclear 3d complexes with only a few exceptions.[10]

Table 2. Experimentally determined spectroscopic parameters of **Fe(L)Cl**, **Fe(L)Br** and **Fe(L)I**

	Fe(L)Cl	Fe(L)Br	Fe(L)I
ΔE_Q (mm.s^{-1})	2.82	3.00	3.14
δ (mm.s^{-1})	0.46	0.44	0.42
D (cm^{-1}) [a]	3.7	5.2	11.5
E/D [b]	0.18	0.13	0.12
g [a]	2.10	2.05	2.08

[a] by SQUID measurements; [b] by EPR spectroscopy.

The ZFS parameters of the three complexes were calculated in the framework of the coupled-perturbed DFT approach (CP-DFT)[11], (Table 3). The influence of the level of theory and comparison with data obtained with LF-DFT[12] are provided as Supporting Information (see S4). Experimental and calculated D values are in a good agreement concerning both their magnitude and sign. While predicted D values are in good agreement with the experimental data, the calculated E/D values display significant deviation, as often observed in a DFT framework.[13] Generally, the main factor driving the magnetic anisotropy is the spin−orbit coupling (SOC). Interestingly, the trend in magnetic anisotropy is seen where D is decomposed into its SOC (D_{SOC}) and spin–spin dipolar contribution (D_{SSC}) terms using CP-DFT (Table 3). As expected, D_{SOC} dominates over D_{SSC}. The contribution of D_{SSC} is not negligible in the case of **Fe(L)Cl** (around 13% of the total D) but decreases from **Fe(L)Cl** to **Fe(L)I**. The importance of dominant D_{SOC} contribution increases from the chlorido to the iodido metal complexes, explaining the observed trend in D values. In an attempt to rationalize the origin of the difference in D_{SOC} between the three complexes, D_{SOC} is

further decomposed into four terms according to single electron excitations: α→α - from singly occupied molecular orbitals (SOMO) to the virtual orbitals (VMOs); β→β - from doubly occupied orbitals (DOMO) to SOMO; α→β – spin flip between SOMOs; β→α – from DOMO to VMO. The first two contributions arise from excitations that lead to S=3/2 excited states, the third to S=1/2 excited states, and the last to S=5/2 excited states. In the case of **Fe(L)Br**, excitations to both doublet and quartet states contribute to D_{SOC}, while for **Fe(L)Cl** and **Fe(L)I** excitations to doublets represent the main contribution. Besides, it should be noted that in the iodido and chlorido complexes the first excited states differ being $S = 5/2$ and $S = 1/2$, respectively (Table S3.1). These data can be thus related to a larger D_{SOC} (αβ) magnitude for **Fe(L)I** with respect to that of **Fe(L)Cl**.
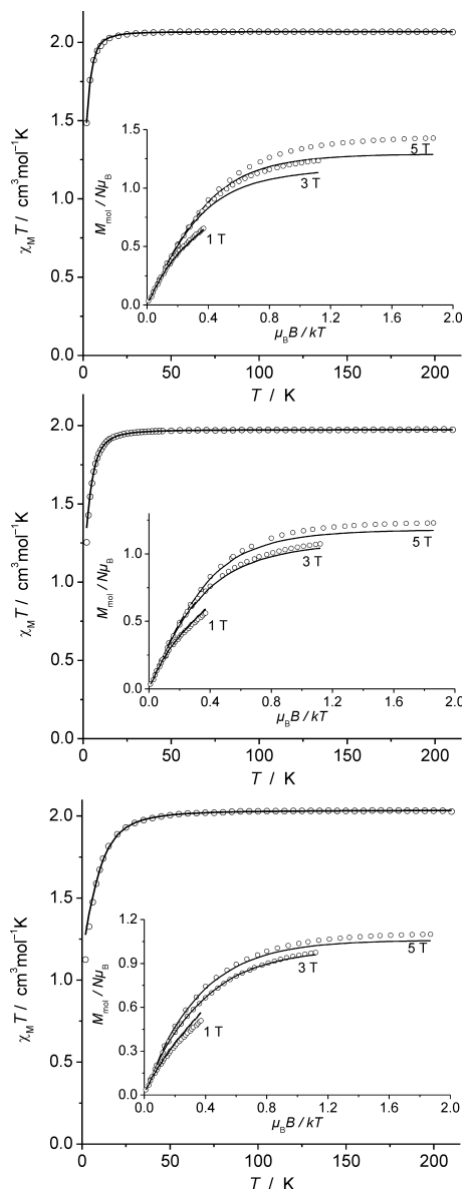

Figure 1. $\chi_M T$ versus T plot for **Fe(L)Cl** (top), **Fe(L)Br** (middle) and **Fe(L)I** (bottom). The insets show variable temperature–variable (VTVH) magnetization measurements as M_{mol} versus $\mu_B B/kT$. Solid lines represent the calculated curve fits (see text).

COMMUNICATION

Table 3. Calculated Mössbauer and ZFS Parameters of **Fe(L)Cl**, **Fe(L)Br** and **Fe(L)I** and decomposition of *D* parameter into various contributions

	Fe(L)Cl	Fe(L)Br	Fe(L)I
ΔE_Q (mm.s⁻¹)	2.74	2.82	2.85
δ (mm.s⁻¹)	0.43	0.42	0.41
D (cm⁻¹)	2.34	4.72	12.42
E/D	0.17	0.06	0.32
D_{SSC} (cm⁻¹)	0.26	0.13	0.00
D_{SOC} (cm⁻¹)	2.08	4.59	12.42
$D_{SOC}(\alpha\alpha)$ (cm⁻¹)	0.33	0.51	-0.63
$D_{SOC}(\beta\beta)$ (cm⁻¹)	0.45	2.01	-1.67
$D_{SOC}(\alpha\beta)$ (cm⁻¹)	1.70	1.64	18.19
$D_{SOC}(\beta\alpha)$ (cm⁻¹)	-0.42	0.43	-3.47
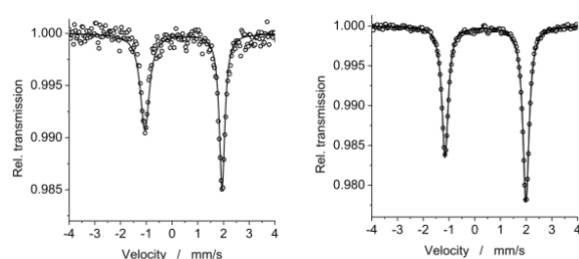
Figure 2. Mössbauer spectra of solid samples of **Fe(L)Br** (left) and **Fe(L)I** (right) recorded at 80 K.

Zero-field powder Mössbauer spectra recorded at 80 K (Table 2, Figure 2) show that the quadrupole splitting (ΔE_Q values) is sensitive to the nature of the coordinating halide, with increasing values from **Fe(L)Cl** to **Fe(L)I**. By contrast the isomer shift δ is comparable for all complexes (0.42-0.46 mm.s⁻¹) and in the expected range for an intermediate spin ground state. The slight decrease of δ upon going from **Fe(L)Cl** to **Fe(L)I**, which reflects different s-electron density at the nucleus, is consistent with the more covalent character of the Fe-X bond for heavier halides. These values are corroborated by DFT calculations (Table 3).

In summary, the present combined experimental and theoretical approach enables the rationalization of experimental data leading to a more complete understanding of the electronic structure of such systems and of the factors that govern the contribution of the different excited spin states in the magnetic anisotropy of intermediate spin state Fe^{III} complexes. The origin of the magnetic anisotropy, and even the trend in values, differs from our earlier studies on the same ligand system with Co^{III} (S=1),[10e] and different complexes with S = 3/2 (Mn^{IV}),[13c] which is a clear indication that any change induces different magnetic behavior depending on the spin system and analogies cannot be drawn a priori with systems that are yet to be investigated. Understanding of these effects and the potential for DFT methods to predict them, opens new opportunities in the rational design of magnetic materials with desired properties.

Experimental Section

General. The syntheses of H₂L^{N2S2} [4] and **Fe^{II}₂SS** are reported elsewhere.[5] Cw-X-band electron paramagnetic resonance (EPR) spectra were recorded with a Bruker EMX, equipped with an Oxford Instruments ESR-900 continuous-flow helium cryostat and an ER-4116 DM Bruker cavity for the 4.5 K experiments. Cw-Q-band EPR spectra were recorded on the same spectrometer equipped with an ER-5106

QTW Bruker cavity. All spectra were recorded at 7K on powder samples. Temperature-dependent magnetic susceptibility measurements were carried out with a *Quantum-Design* MPMS-XL-5 SQUID magnetometer, and Mössbauer spectra were recorded with a ⁵⁷Co source in a Rh matrix using an alternating constant-acceleration Wissel Mössbauer spectrometer operated in the transmission mode and equipped with a Janis closed-cycle helium cryostat; further details can be found in the SI.

Synthesis of Fe(L)Br. Solid NaH (60% in mineral oil, 14 mg, 0.3 mmol) was added to the solution of H₂L^{N2S2} (50 mg, 0.086 mmol) in THF (2 mL) at 293 K. After 20 min, the excess NaH was removed by filtration and a solution of FeBr₃ (28 mg, 0.095 mmol) in THF (3 mL) was added to the yellow solution under stirring. During the addition, the color of the solution turned to red, and subsequently to deep red. A brown-red precipitate formed over several few minutes. The mixture was stirred for 1 h. The precipitate was isolated and redissolved in dichloromethane and subsequently filtered to remove residual solid. The solvent was removed from the filtrate in vacuo and the residual solid dried and collected as a deep red powder (39mg, 63.4%). Single crystals suitable for X-ray diffraction analysis were obtained by slow diffusion of diethyl ether into the solution of the product in CH₂Cl₂:CH₃CN (4:1) at 293 K.

Synthesis of Fe(L)I. Solid *n*-tetrabutylammonium iodide (44 mg, 0.119 mmol) was added to a suspension of the dinuclear [Fe^{II}₂(LSSL)](ClO₄)₂ **Fe^{II}SS** (35 mg, 0.024 mmol) in CH₃CN (10 mL). After few min, a brown precipitate was formed. After stirring for 1h, the solid was isolated by filtration, washed with MeCN, dried under vacuum and collected as dark brown powder (32 mg, 0.042 mmol, 88%). X-ray suitable single crystals of **Fe(L)I** were obtained by slow diffusion of diethyl ether into the solution of the product in CH₂Cl₂:CH₃CN (4:1) at 293 K.

Computational details. Density Functional Theory (DFT) calculations, using Amsterdam Density Functional program package (ADF2016)[14]. In first step geometry optimizations were performed using two general gradient approximations (GGA) in the form of OPBE[15] and S12g[16]. Scalar relativistic corrections have been included self-consistently in all calculations by using the zeroth-order regular approximation (ZORA)[17]. Optimizations of all spin states for three complexes under investigation were performed by letting the structure of each spin state relax towards its own equilibrium geometry separately. Molecular orbitals were expanded in an uncontracted set of Slater type orbitals (STOs) of triple-zeta quality with two polarization function (TZ2P)[18] full electron basis set. All calculations were done in a spin-unrestricted fashion; the very good Becke grid was used. Calculations of ZFS were performed on the experimentally determined X-ray structures using coupled perturbed SOC DFT method at BP86[19] ZORA-def2-TZVP[20] level of theory, as implemented in ORCA (version 4.0.1.2)[21]. Mössbauer parameters have been calculated at OPBE/TZP level of theory according to the procedure by Noodleman et al..[22] Further details are provided in S4.

[1]   a) S. Mossin, B. L. Tran, D. Adhikari, M. Pink, F. W. Heinemann, J. Sutter, R. K. Szilagyi, K. Meyer, D. J. Mindiola, *J. Am. Chem. Soc.* **2012**, *134*, 13651-13661; b) B. Djukic, P. A. Dube, F. Razavi, T. Seda, H. A. Jenkins, J. F. Britten, M. T. Lemaire, *Inorg. Chem.* **2009**, *48*, 699-707; c) M. Nakamura, *Coord. Chem. Rev.* **2006**, *250*, 2271-2294; d) E. Edler, M. Stein, *Eur. J. Inorg. Chem.* **2014**, *2014*, 3587-3599; e) S. A. Cook, D. C. Lacy, A. S. Borovik, in *Spin States in Biochemistry*

COMMUNICATION

and Inorganic Chemistry, John Wiley & Sons, Ltd, **2015**, pp. 203-227.

[2] a) M. Nakano, H. Oshio, *Chem. Soc. Rev.* **2011**, *40*, 3239-3248; b) W. O. Koch, V. Schünemann, M. Gerdan, A. X. Trautwein, H.-J. Krüger, *Chem. Eur. J.* **1998**, *4*, 686-691; c) D. Sakow, D. Baabe, B. Böker, O. Burghaus, M. Funk, C. Kleeberg, D. Menzel, C. Pietzonka, M. Bröring, *Chem. Eur. J.* **2014**, *20*, 2913-2924.

[3] a) H. Keutel, I. Käpplinger, E. G. Jäger, M. Grodzicki, V. Schünemann, A. X. Trautwein, *Inorg. Chem.* **1999**, *38*, 2320-2327; b) H. Jacobsen, J. P. Donahue, *Inorg. Chem.* **2008**, *47*, 10037-10045; c) C. H. Chang, A. J. Boone, R. J. Bartlett, N. G. J. Richards, *Inorg. Chem.* **2004**, *43*, 458-472.

[4] M. A. Kopf, D. Varech, J. P. Tuchagues, D. Mansuy, I. Artaud, *J. Chem. Soc., Dalton Trans.* **1998**, 991-998.

[5] *The synthesis of this dinuclear will be described in a forthcoming publication.*

[6] M. Swart, A. W. Ehlers, K. Lammertsma, *Mol. Phys.* **2004**, *102*, 2467-2474.

[7] M. Swart, *Chem. Phys. Lett.* **2013**, *580*, 166-171.

[8] M. Swart, M. Gruden, *Acc. Chem. Res.* **2016**, *49*, 2690-2697.

[9] a) C. Duboc, T. Phoeung, S. Zein, J. Pécaut, M.-N. Collomb, F. Neese, *Inorg. Chem.* **2007**, *46*, 4905-4916; b) H. I. Karunadasa, K. D. Arquero, L. A. Berben, J. R. Long, *Inorg. Chem.* **2010**, *49*, 4738-4740; c) C. Mantel, C. Baffert, I. Romero, A. Deronzier, J. Pécaut, M.-N. Collomb, C. Duboc, *Inorg. Chem.* **2004**, *43*, 6455-6463; d) M. R. Saber, K. R. Dunbar, *Chem. Commun.* **2014**, *50*, 12266-12269; e) J. Krzystek, S. A. Zvyagin, A. Ozarowski, A. T. Fiedler, T. C. Brunold, J. Telser, *J. Am. Chem. Soc.* **2004**, *126*, 2148-2155; f) F. Yang, Q. Zhou, Y. Zhang, G. Zeng, G. Li, Z. Shi, B. Wang, S. Feng, *Chem. Commun.* **2013**, *49*, 5289-5291; g) R. Boča, J. Miklovič, J. Titiš, *Inorg. Chem.* **2014**, *53*, 2367-2369.

[10] a) J. Krzystek, A. Ozarowski, S. A. Zvyagin, J. Telser, *Inorg. Chem.* **2012**, *51*, 4954-4964; b) S. Ye, F. Neese, *J. Chem. Theory Comput.* **2012**, *8*, 2344-2351; c) S. Mossin, H. Weihe, A.-L. Barra, *J. Am. Chem. Soc.* **2002**, *124*, 8764-8765; d) P. J.

Desrochers, J. Telser, S. A. Zvyagin, A. Ozarowski, J. Krzystek, D. A. Vicic, *Inorg. Chem.* **2006**, *45*, 8930-8941; e) D. Brazzolotto, M. Gennari, S. Yu, J. Pécaut, M. Rouzières, R. Clérac, M. Orio, C. Duboc, *Chem. Eur. J.* **2016**, *22*, 925-933.

[11] F. Neese, E. I. Solomon, *Inorg. Chem.* **1998**, *37*, 6568-6582.

[12] M. Atanasov, C. A. Daul, *Chem. Phys. Lett.* **2003**, *381*, 584-591.

[13] a) F. Neese, *J. Am. Chem. Soc.* **2006**, *128*, 10213-10222; b) C. Duboc, D. Ganyushin, K. Sivalingam, M.-N. Collomb, F. Neese, *J. Phys. Chem. A* **2010**, *114*, 10750-10758; c) M. Zlatar, M. Gruden, O. Y. Vassilyeva, E. A. Buvaylo, A. N. Ponomarev, S. A. Zvyagin, J. Wosnitza, J. Krzystek, P. Garcia-Fernandez, C. Duboc, *Inorg. Chem.* **2016**, *55*, 1192-1201.

[14] a) G. te Velde, F. M. Bickelhaupt, E. J. Baerends, C. Fonseca Guerra, S. J. A. van Gisbergen, J. G. Snijders, T. Ziegler, *J. Comput. Chem.* **2001**, *22*, 931-967; b) C. C. Pye, T. Ziegler, *Theor. Chem. Acc.* **1999**, *10*.

[15] M. Swart, A. W. Ehlers, K. Lammertsma, *Mol. Phys.* **2004**, *102*, 2467-2474.

[16] M. Swart, *Chem. Phys. Lett.* **2013**, *580*, 166-171.

[17] a) E. v. Lenthe, A. Ehlers, E.-J. Baerends, *J. Chem. Phys.* **1999**, *110*, 8943-8953; b) E. v. Lenthe, E. J. Baerends, J. G. Snijders, *J. Chem. Phys.* **1994**, *101*, 9783-9792.

[18] a) E. van Lenthe, E. J. Baerends, *J. Comput. Chem.* **2003**, *24*, 1142-1156; b) D. P. Chong, E. Van Lenthe, S. Van Gisbergen, E. J. Baerends, *J. Comput. Chem.* **2004**, *25*, 1030-1036.

[19] a) A. D. Becke, *Phys. Rev. A* **1988**, *38*, 3098-3100; b) J. P. Perdew, *Phys. Rev. B* **1986**, *34*, 7406-7406; c) J. P. Perdew, *Phys. Rev. B* **1986**, *33*, 8822-8824.

[20] a) F. Weigend, R. Ahlrichs, *Phys. Chem. Chem. Phys.* **2005**, *7*, 3297-3305; b) D. A. Pantazis, F. Neese, *J. Chem. Theory Comput.* **2009**, *5*, 2229-2238.

[21] F. Neese, *Wiley Interdisciplinary Reviews: Computational Molecular Science* **2012**, *2*, 73-78.

[22] G. M. Sandala, K. H. Hopmann, A. Ghosh, L. Noodleman, *J. Chem. Theory Comput.* **2011**, *7*, 3232-3247.

COMMUNICATION

Entry for the Table of Contents

COMMUNICATION
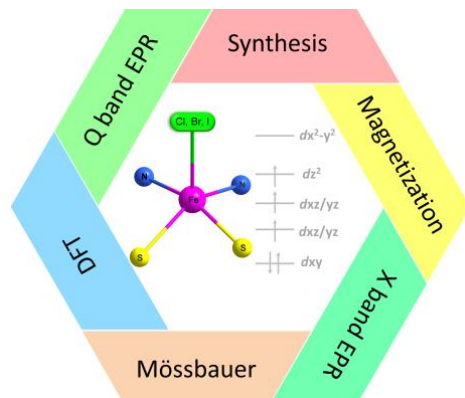
Effect of halide ligands on the magnetic anisotropy in a series of square pyramidal Fe(III) complexes with an S = 3/2 ground state.

Lianke Wang, Matija Zlatar, Filip Vlahović, Serhiy Demeshko, Christian Philouze, Florian Molton, Marcelllo Gennari, Franc Meyer, Carole Duboc* and Maja Gruden*

Page No. – Page No.

Experimental and Theoretical Identification of the Origin of Magnetic Anisotropy in Intermediate Spin Iron(III) Complexes.

Accepted Manuscript